

On the Accuracy of Averaging Radar Backscattering Coefficients for Bare Soils Using the Finite-Element Method

Uday K. Khankhoje, Mariko Burgin, *Student Member, IEEE*, and Mahta Moghaddam, *Fellow, IEEE*

Abstract—Radar backscattering coefficients for heterogeneous pixels are traditionally assumed to be the average of the coefficients for the constitutive homogeneous pixels. We investigate the validity of this assumption for bare rough surfaces by using the 2-D finite-element method to compute the ensemble averaged “true” coefficients for heterogeneous pixels and compare these values with the computed averages for a variety of surfaces. We quantify the impact of heterogeneity in both soil moisture and surface roughness on the averaging assumption. We find that the validity of the assumption rests crucially on the surface correlation type (exponential or Gaussian) and length. In particular, when considering pixels with either heterogeneous soil moisture or roughness, we find that for high-contrast pixels, the backscatter averaging assumption breaks down by as much as 11 dB for Gaussian correlated surfaces for the longest correlation lengths considered (regardless of the source of heterogeneity), whereas for exponentially correlated surfaces, it breaks down by 6 dB for pixels with heterogeneous roughness and 2 dB for pixels with heterogeneous moisture. We attribute this behavior to Gaussian correlated surfaces possessing higher cross-pixel coherent interactions. Furthermore, conditions of validity for the backscatter averaging assumption are identified.

Index Terms—Electromagnetic scattering by rough surfaces, finite-element methods (FEMs).

I. INTRODUCTION

RADAR data, such as data provided by synthetic aperture radar (SAR) systems, are available at various spatial scales. Examples for high-resolution spaceborne radars are the Japanese Earth Resources Satellite and the Advanced Land Observing Satellite Phased Array type L-band SAR (PALSAR), which have provided data at the resolution scales of 10–100 m. An example for a high-resolution airborne radar is the Airborne Microwave Observatory for Subsurface and Subcanopy (AirMOSS) mission radar capable of producing radar backscattering coefficients in the 10–100-m resolution range [1]. A coarser scale radar data product will be delivered by the Soil Moisture Active Passive mission to be launched in October 2014 [2], delivering a radar data product at 3-km resolution.

Manuscript received June 17, 2013; revised September 14, 2013 and October 28, 2013; accepted November 27, 2013.

U. K. Khankhoje and M. Moghaddam are with the Ming Hsieh Department of Electrical Engineering, University of Southern California, Los Angeles, CA 90089 USA (e-mail: uday@alumni.caltech.edu).

M. Burgin is with the Department of Electrical Engineering and Computer Science, University of Michigan, Ann Arbor, MI 48109 USA.

Digital Object Identifier 10.1109/LGRS.2013.2293392

In this letter, we focus on soil moisture as the variable of interest to be observed through radar backscattering coefficient measurements. Most traditional radar retrieval techniques employ forward models that make the assumption of scene homogeneity. The assumption of a homogeneous scene over coarse-scale radar pixels can significantly impact the retrieval accuracy of soil moisture and needs to be investigated. This can be achieved by breaking a heterogeneous scene down into smaller subpixels to which the homogeneous assumption can be applied. For each of these subpixels, the radar backscattering coefficients can be simulated separately. Airborne or spaceborne measurements over such a coarse-scale pixel are an aggregate of the contributions of a potentially large set of scatterer distributions within that pixel. This highlights the need to study spatial up- and downscaling techniques using radar forward models that are capable of handling finer scale scene heterogeneity within a coarse resolution pixel to achieve higher accuracy in soil moisture retrieval at the coarse scale [3]. The task of soil moisture retrieval from remotely sensed data is further complicated when variability in landscape, topography, and soil texture is introduced. Furthermore, hydrologic models that ingest soil moisture information determined from remotely sensed data generally require inputs at coarser scales such as kilometer scale.

A commonly used technique for achieving upscaling is a simple weighted averaging of the radar backscattering coefficients over a set of adjacent (high-resolution) pixels (these weights could correspond to the area fraction of each pixel, for instance, [4]). Physically, this corresponds to averaging the received power from each of the constitutive pixels. Experimentally and via numerical simulations [4], [5], it is known that radar backscattering coefficients over bare soil surfaces are nonlinear functions of soil moisture and surface statistics. Thus, for backscatter averaging to accurately represent average soil moisture, two conditions must be met: 1) There should be minimal coherent interaction between constitutive pixels; and (2) the interpixel variability of physical parameters such as soil moisture or surface roughness should be small enough such that spatially, the backscattering coefficients behave approximately linearly over this restricted range of parameters. The latter assumption often holds true because soil parameters are not likely to vary very sharply between adjacent pixels.

In this letter, speckle is assumed to be reduced by multilooking first. The resulting speckle-free pixels are then investigated for the validity of the backscatter averaging assumption for bare

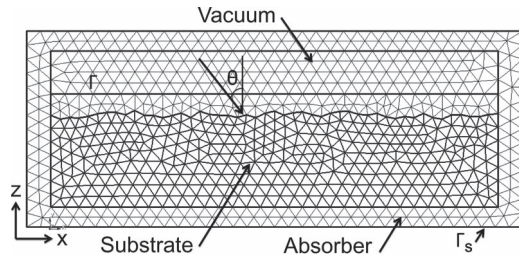


Fig. 1. Tesselated computational domain, with Γ_s denoting the outermost boundary on which the radiation boundary condition is applied and Γ denoting the integration contour from which the far field is calculated. The soil and vacuum subdomains are 80λ in width and have average heights of 3.25λ and 2.75λ , respectively. An adiabatic absorber of thickness λ frames the computational domain. Incidence angle $\theta = 40^\circ$, and wavelength $\lambda = 0.69$ m.

soils over heterogeneous scenes. We discuss certain scenarios where the assumption breaks and provide relevant analytical justifications. Essential to this investigation is the ability to compare averages of backscattering coefficients with “true” values. We use a 2-D finite-element method (FEM) [5] to simulate the backscattering coefficient from a heterogeneous pixel and use this as our “truth.” The FEM offers considerable flexibility in being able to specify a heterogeneous scattering substrate, a distinct advantage over other methods such as the method of moments or the small perturbation method (SPM).

The layout of this letter is as follows. First, the FEM is briefly described; next, simulation results for a variety of different scattering configurations are provided; and finally, the results are interpreted in the context of examining the validity of estimating the true backscattering coefficients via an averaging operation.

II. FEM

The FEM tool that we use is based on our recently developed 2-D vector-element-based FEM built for the purpose of computing rough surface scattering [5]. A schematic of the computational domain and associate simulation parameters are shown in Fig. 1. Three enhancements improve the accuracy and computation speed of the method over a standard FEM.

- 1) We move from a total-field formulation to a scattered-field formulation. As reported in the context of a time-domain FEM [6], this formulation leads to the variable of interest being the scattered field in the air domain, and the total field in the soil domain. As a result, the incident field is introduced into the formulation at the interface between the air and soil domains. This is already an improvement over the total-field formulation, where the incident field is introduced on the outer boundary of the air domain and suffers dispersion errors as it propagates through the finite-element mesh to the air–soil interface.
- 2) We incorporate a wavelength-thick layer of an adiabatic absorber just inside the mesh boundaries. The essential idea [7] in such an absorber is that the loss is turned on gradually (such as a quadratic function of distance from an interface), which leads to a smaller reflection from the layer, as compared with the case of an absorber with spatially homogeneous loss. To be more clear, consider an

interface between air and the absorber of thickness L at a plane given by $x = 0$. With the absorber on the right, the complex refractive index n takes on the following form: $n = 1 - j(5/k)(x/L)^2$ for $0 \leq x \leq L$, where k is the free-space wave vector. As in [5], we apply the radiation boundary condition on the outermost mesh boundaries (see contour Γ_s in Fig. 1).

- 3) We apply our recently developed mesh-reconfiguration technique [8], which facilitates Monte Carlo computations with a single mesh, resulting in a fourfold improvement in computational runtime over other methods that generate a new mesh for each instance of a rough surface.

To specify the permittivity of each finite element, we use a microwave-dielectric model [9] to infer the soil permittivity as a function of soil bulk density, percentage sand and clay, and moisture. We specify the following constants: water temperature: 10°C ; water salinity: 4 g salt/kg water; specific density of solid soil particles: $\rho_s = 2.66$ g/cm³; empirically determined constant: $\alpha = 0.65$. We consider a four-layer soil, which has the following specifications (from top to bottom, per layer): density (in grams per cubic centimeter): 1.46, 1.5, 1.62, and 1.61; sand (in percentage): 11.4, 11.4, 7.3, and 11.4; clay (in percentage): 20.5, 20.5, 27.5, and 20.5; and depth (in meters): 0.3, 0.26, 0.3, ∞ .

III. SIMULATIONS

A. Strategy

For the purpose of scattering simulations, we consider surfaces with either Gaussian or exponential correlation statistics, as well as a wide range of correlation lengths, soil moisture values, and root-mean-square (RMS) surface roughness. Specifically, a homogeneous pixel has a parameter picked from each of the following sets: correlation length $\mathcal{L} = \{2.4, 4.8, 7.2\}$ (in terms of kl); soil moisture $\mathcal{M} = \{5\%, 15\%, 35\%\}$ (percentage soil moisture); and roughness $\mathcal{H} = \{0.1, 0.4, 0.8\}$ (in terms of kh), where $k = 2\pi/\lambda$ is the free-space wavenumber for a wavelength λ , and l and h are the surface RMS height and correlation length, respectively.

A pixel with heterogeneous moisture is composed by picking an element each from \mathcal{L} and \mathcal{H} and two or three elements from \mathcal{M} . A pixel with heterogeneous roughness is composed by picking an element each from \mathcal{L} and \mathcal{M} and two elements from \mathcal{H} . In a heterogeneous pixel, the constitutive (homogeneous) pixels are horizontally arranged, and their spatial order is randomized. The computation of backscattering coefficients involves taking an ensemble average over 75 different surface realizations. It must be noted that the standard deviation observed in the backscattering coefficients after ensemble averaging is on the order of 0.6 dB. We determine both the copolarized backscattering coefficients, i.e., HH and VV (H: horizontally polarized; V: vertically polarized); since the method is 2-D, cross-polarized quantities cannot be determined.

B. Results

In Table I, we present sample results for pixels with heterogeneity in moisture (left) and roughness (right), displaying the

TABLE I

COMPARISON OF FEM-COMPUTED VV-POL RADAR BACKSCATTER IN DECIBELS FROM GAUSSIAN (G) VERSUS EXPONENTIAL (E) CORRELATED ROUGH SOIL SURFACES AT $\theta = 40^\circ$ (FROM NORMAL). PIXELS w (WET) AND d (DRY) REFER TO HOMOGENEOUS PIXELS WITH 35% AND 5% SOIL MOISTURE, RESPECTIVELY, WHEREAS wd REFERS TO A HETEROGENEOUS PIXEL COMPOSED OF w AND d , AND \overline{wd} CORRESPONDS TO THE AVERAGE OF w AND d . IN THESE PIXELS (LEFT HALF) THE HOMOGENEOUS ROUGHNESS IS $kh = 0.1$. PIXELS s (SMOOTH) AND r (ROUGH) REFER TO HOMOGENEOUS PIXELS WITH ROUGHNESS $kh = 0.1$ AND $kh = 0.8$, RESPECTIVELY, WHEREAS sr REFERS TO A HETEROGENEOUS PIXEL COMPOSED OF s AND r , AND \overline{sr} CORRESPONDS TO THE AVERAGE OF s AND r . IN THESE PIXELS (RIGHT HALF) THE HOMOGENEOUS SOIL MOISTURE IS 35%. ALL AVERAGES ARE TAKEN IN THE LINEAR SCALE

	2.4	4.8	7.2	$\frac{kl}{\lambda}$	2.4	4.8	7.2	
w	-21.0	-36.5	-36.3	G	-21.0	-36.5	-36.3	s
d	-27.8	-38.4	-39.4		-4.3	-15.4	-28.2	r
wd	-22.2	-29.8	-29.6		-7.8	-14.4	-19.3	sr
\overline{wd}	-23.2	-37.3	-37.6		-7.2	-18.4	-30.6	\overline{sr}
w	-20.6	-23.3	-24.1	E	-20.6	-23.3	-24.1	s
d	-26.1	-29.4	-29.7		-3.8	-14.2	-10.3	r
wd	-21.9	-24.6	-24.9		-8.4	-10.5	-8.6	sr
\overline{wd}	-22.5	-25.4	-26.1		-6.7	-16.7	-13.1	\overline{sr}

TABLE II

FEM-COMPUTED HH- AND VV-POL BACKSCATTER RESULTS IN DECIBELS FOR EXPONENTIALLY CORRELATED SOILS. PIXELS w (WET), m (MEDIUM), AND d (DRY) REFER TO HOMOGENEOUS PIXELS WITH 35%, 15%, AND 5% SOIL MOISTURE, RESPECTIVELY, WHEREAS wd REFERS TO A HETEROGENEOUS PIXEL COMPOSED OF w AND d , AND \overline{wd} CORRESPONDS TO THE AVERAGE OF w AND d , TAKEN IN THE LINEAR SCALE

$kl \rightarrow$		2.4		4.8		7.2	
$\downarrow kh$		HH	VV	HH	VV	HH	VV
0.1	w	-23.7	-20.6	-26.7	-23.3	-27.3	-24.1
	m	-25.1	-23.1	-28.2	-26.0	-28.6	-26.8
	d	-26.8	-26.1	-30.1	-29.4	-29.9	-29.7
	wd	-25.3	-21.9	-26.5	-24.6	-27.0	-24.9
	\overline{wd}	-25.0	-22.5	-28.1	-25.4	-28.4	-26.1
	\overline{wmd}	-25.6	-24.0	-28.7	-26.7	-28.5	-26.8
0.4	w	-13.9	-9.7	-16.5	-12.6	-17.6	-13.7
	m	-15.7	-12.7	-18.5	-15.5	-19.5	-16.8
	d	-17.9	-16.5	-20.5	-19.0	-21.6	-20.5
	wd	-15.2	-11.7	-17.2	-14.2	-18.8	-15.4
	\overline{wd}	-15.5	-11.9	-18.1	-14.7	-19.2	-15.9
	\overline{wmd}	-15.8	-12.9	-18.4	-15.6	-19.5	-16.9
0.8	w	-5.6	-3.8	-16.3	-14.2	-13.1	-10.3
	m	-8.0	-6.6	-18.7	-16.9	-15.4	-13.4
	d	-11.2	-10.2	-21.9	-20.5	-18.3	-17.0
	wd	-7.8	-5.9	-18.0	-15.9	-14.9	-11.8
	\overline{wd}	-7.6	-5.9	-18.3	-16.3	-15.0	-12.5
	\overline{wmd}	-8.2	-6.8	-19.6	-17.9	-15.5	-13.5
		-7.7	-6.1	-18.4	-16.5	-15.1	-12.8

backscattering coefficients for a range of correlation lengths and fixed roughness and moisture, respectively, and for both surface correlation types. A complete set of results is presented in Tables II–V.

TABLE III

FEM-COMPUTED HH- AND VV-POL BACKSCATTER RESULTS IN DECIBELS FOR GAUSSIAN CORRELATED SOILS. LEGENDS CARRY THE SAME MEANING AS IN THE CAPTION OF TABLE II

$kl \rightarrow$		2.4		4.8		7.2	
$\downarrow kh$		HH	VV	HH	VV	HH	VV
0.1	w	-25.3	-21.0	-36.1	-36.5	-35.4	-36.3
	m	-27.3	-24.1	-36.7	-37.1	-36.7	-38.3
	d	-29.9	-27.8	-37.6	-38.4	-37.6	-39.4
	wd	-26.4	-22.2	-30.9	-29.8	-31.0	-29.6
	\overline{wd}	-27.0	-23.2	-36.8	-37.3	-36.4	-37.6
	\overline{wmd}	-27.8	-24.6	-36.6	-37.2	-36.4	-38.0
0.4	w	-13.2	-9.0	-28.6	-25.3	-39.6	-38.5
	m	-15.4	-12.1	-30.9	-28.0	-40.9	-41.0
	d	-18.3	-15.9	-34.0	-31.5	-42.3	-43
	wd	-15.8	-11.3	-28.6	-25.5	-32.0	-30.2
	\overline{wd}	-15.0	-11.2	-30.5	-27.4	-40.7	-40.2
	\overline{wmd}	-15.5	-12.2	-30.8	-28.1	-40.7	-40.5
0.8	w	-7.4	-4.3	-17.0	-15.4	-29.5	-28.2
	m	-10.0	-7.5	-19.4	-18.1	-31.9	-30.8
	d	-13.2	-11.3	-22.7	-21.7	-35.0	-34.4
	wd	-9.1	-6.9	-18.6	-17.0	-28.1	-27.2
	\overline{wd}	-9.4	-6.5	-19.0	-17.5	-31.4	-30.3
	\overline{wmd}	-10.4	-7.8	-19.4	-18.1	-31.9	-31.0
		-9.6	-6.8	-19.1	-17.7	-31.6	-30.4

TABLE IV

FEM-COMPUTED HH- AND VV-POL BACKSCATTER RESULTS IN DECIBELS FOR EXPONENTIALLY CORRELATED SOILS. PIXELS s (SMOOTH), i (INTERMEDIATE), AND r (ROUGH) REFER TO HOMOGENEOUS PIXELS WITH $kh = 0.1$, 0.4, AND 0.8 SURFACE ROUGHNESS, RESPECTIVELY, WHEREAS si REFERS TO A HETEROGENEOUS PIXEL COMPOSED OF s AND i , AND \overline{si} CORRESPONDS TO THE AVERAGE OF s AND i , TAKEN IN THE LINEAR SCALE

$kl \rightarrow$		2.4		4.8		7.2	
$\downarrow mv$		HH	VV	HH	VV	HH	VV
5%	s	-26.8	-26.1	-30.1	-29.4	-29.9	-29.7
	i	-17.9	-16.5	-20.5	-19.0	-21.6	-20.5
	r	-11.2	-10.2	-21.9	-20.5	-18.3	-17.0
	si	-20.3	-18.8	-22.2	-19.2	-23.7	-20.9
	\overline{si}	-20.4	-19.1	-23.1	-21.6	-24.0	-23.0
	sr	-16.2	-16.0	-17.3	-16.2	-18.7	-16.9
15%	s	-25.1	-23.1	-28.2	-26.0	-28.6	-26.8
	i	-15.7	-12.7	-18.5	-15.5	-19.5	-16.8
	r	-8.0	-6.6	-18.7	-16.9	-15.4	-13.4
	si	-18.3	-15.3	-19.8	-17.4	-21.6	-18.2
	\overline{si}	-18.2	-15.3	-21.1	-18.1	-22.0	-19.4
	sr	-13.4	-12.8	-15.2	-13.0	-14.7	-13.4
35%	s	-23.7	-20.6	-26.7	-23.3	-27.3	-24.1
	i	-13.9	-9.7	-16.5	-12.6	-17.6	-13.7
	r	-5.6	-3.8	-16.3	-14.2	-13.1	-10.3
	si	-17.6	-13.2	-18.5	-13.2	-19.7	-16.8
	\overline{si}	-16.5	-12.4	-19.1	-15.3	-20.2	-16.3
	sr	-11.0	-8.4	-12.2	-10.5	-10.3	-8.6
		-8.6	-6.7	-18.9	-16.7	-15.9	-13.1

TABLE V
FEM-COMPUTED HH- AND VV-POL BACKSCATTER RESULTS IN DECIBELS FOR GAUSSIAN CORRELATED SOILS. LEGENDS CARRY THE SAME MEANING AS IN THE CAPTION OF TABLE IV

$kl \rightarrow$		2.4		4.8		7.2	
$\downarrow mv$		HH	VV	HH	VV	HH	VV
5%	s	-29.9	-27.8	-37.6	-38.4	-37.6	-39.4
	i	-18.3	-15.9	-34.0	-31.5	-42.3	-43.0
	r	-13.2	-11.3	-22.7	-21.7	-35.0	-34.4
	si	-21.1	-19.1	-29.8	-27.5	-33.6	-32.0
	\overline{si}	-21.0	-18.6	-35.4	-33.7	-39.3	-40.8
	sr	-14.9	-13.9	-21.8	-20.2	-28.9	-26.7
	\overline{sr}	-16.1	-14.2	-25.6	-24.6	-36.1	-36.2
	15%	s	-27.3	-24.1	-36.7	-37.1	-36.7
i		-15.4	-12.1	-30.9	-28.0	-40.9	-41.0
r		-10.0	-7.5	-19.4	-18.1	-31.9	-30.8
si		-19.1	-15.8	-29.6	-26.0	-32.4	-28.9
\overline{si}		-18.1	-14.8	-32.9	-30.5	-38.3	-39.4
sr		-11.9	-11.0	-18.9	-17.5	-26.0	-21.7
\overline{sr}		-12.9	-10.4	-22.3	-21.1	-33.7	-33.1
35%		s	-25.3	-21.0	-36.1	-36.5	-35.4
	i	-13.2	-9.0	-28.6	-25.3	-39.6	-38.5
	r	-7.4	-4.3	-17.0	-15.4	-29.5	-28.2
	si	-15.9	-11.7	-27.6	-21.9	-31.2	-26.2
	\overline{si}	-16.0	-11.8	-30.9	-28.0	-37.0	-37.3
	sr	-9.7	-7.8	-17.3	-14.4	-24.1	-19.3
	\overline{sr}	-10.4	-7.2	-20.0	-18.4	-31.5	-30.6

An immediate observation for smooth homogeneous pixels (roughness $kh = 0.1$) is that Gaussian and exponentially correlated surfaces display very different behaviors with increasing correlation length, particularly for $kl > 2.4$; while exponential surfaces show a gradual decrease in backscattering coefficients, the corresponding decrease for Gaussian surfaces is much sharper.

When considering high-contrast heterogeneous pixels composed of either a wet and dry pixel (35% and 15% soil moisture, respectively) or a smooth and high-roughness pixel ($kh = 0.1$ and 0.8, respectively), the backscatter averaging assumption is seen to break down for Gaussian correlated surfaces, particularly with increasing correlation lengths. We find that the difference between the “true” and average backscattering coefficients, i.e., $\Delta\sigma_0$, to be approximately 11 dB at the longest correlation length, i.e., $kl = 7.2$. On the other hand, the assumption is found to be accurate to $\Delta\sigma_0 \approx 2$ dB for exponentially correlated surfaces with heterogeneous moisture while breaking down by nearly 6 dB for pixels with heterogeneous roughness.

When the contrast in heterogeneity is not as high, for instance, if a pixel is composed of a wet, medium, and dry pixel (35%, 5%, and 15% soil moisture, respectively) or a smooth and intermediate-roughness pixel ($kh = 0.1, 0.4$, respectively), we find that the “true” and average values agree quite well for both surface correlation types and all correlation lengths considered.

IV. DISCUSSION

To explain the markedly different behavior of Gaussian and exponential surfaces with correlation length, we take recourse

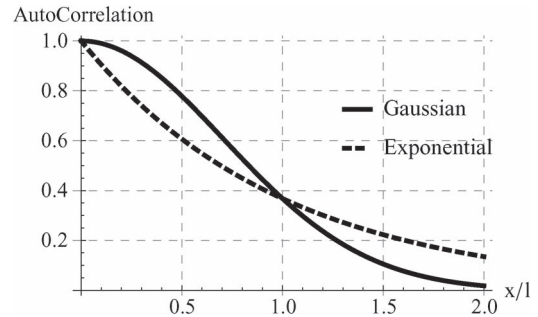


Fig. 2. Plot of the autocorrelation functions for Gaussian and exponential surfaces as a function of x/l .

to the first-order SPM [10]. This semi-analytical method has a limited range of applicability [11], particularly $kh < 0.3$, $s < 0.3$, where s is the RMS slope ($s = \sqrt{2}h/l$ for Gaussian surfaces), and it cannot be used for substrates that are heterogeneous in the horizontal direction. However, owing to its analytical formulation, it is useful in guiding intuition, at least in its domain of applicability. The SPM predicts that the backscattering coefficients from a rough surface are proportional to the roughness spectrum of the surface, i.e., $W(2k \sin \theta)$, where θ is the angle of incidence measured from the normal [5]. This roughness spectrum is the Fourier transform of the surface autocorrelation function $\rho(r)$.

Consider the ratio of the roughness spectra as a function of surface correlation length for two cases, i.e., W_g/W_e , where subscripts g and e refer to Gaussian and exponential surfaces, respectively. We have $W_g = lh^2/(2\sqrt{\pi}) \exp(-k^2l^2/4)$, and $W_e = (lh^2/\pi)/(1 + k^2l^2)$. It is evident that, while W_g and W_e are comparable up to $kl \approx 3$, the ratio drops monotonically and sharply for $kl > 3$. Thus, it comes as little surprise that the two surfaces behave very differently at longer correlation lengths and explains why Gaussian correlated surfaces show lower backscattering coefficients than their exponential counterparts.

We now turn to the central observation of the breakdown of the backscatter averaging assumption with increasing correlation length for high-contrast heterogeneous pixels. It was suggested in the introduction that this assumption will hold only as long as coherent interactions between adjacent pixels are negligible. We now examine the source of coherent interactions by investigating the autocorrelation function for the two surface types. We have $\rho_g(x/l) = \exp(-(x/l)^2)$ and $\rho_e(x/l) = \exp(-|x/l|)$, and these are graphically shown in Fig. 2.

For both of these functions, $\rho(x/l) < 1/e$ for $|x/l| > 1$, and hence, the region where the autocorrelation function becomes significant is for $|x| < l$. As l increases, so does the region $|x|$ where ρ is significant, implying that there will be more cross correlation between adjacent pixels for higher values of l . Next, in this region of significance, it can be seen that $\rho_g > \rho_e$, implying that the strength of interaction between adjacent pixels is higher for Gaussian correlated surfaces. This inference is validated by the simulation results, which show the backscatter averaging assumption to break more severely at higher correlation for high-contrast heterogeneous pixels.

On the inspection of the behavior of backscattering coefficients as a function of surface roughness for pixels with heterogeneous moisture, it can be seen that for exponential surfaces, increasing surface roughness always leads to better agreement between the “true” and average backscattering coefficients. This also holds true for Gaussian surfaces with moderate ($kl \leq 4.8$) correlation lengths. Since each surface is modeled as a *random* process, it is expected that an increase in the surface RMS height will lead to an increase in multiple surface-bounce events of the incident wave, leading to a decrease in coherence between adjacent pixels.

Contrasting the cases of heterogeneous moisture with those of heterogeneous roughness for Gaussian surfaces, we find that on average, soil moisture content has a very weak impact on $\Delta\sigma_0$ when considering heterogeneous roughness (i.e., keep correlation length fixed and examine $\Delta\sigma_0$ by varying moisture in Table V). However, $\Delta\sigma_0$ does show dependence on roughness when considering heterogeneous moisture (i.e., keep correlation length fixed and examine $\Delta\sigma_0$ by varying roughness in Table III). In this respect, roughness is more important in characterizing heterogeneity impact on backscattering coefficients than soil moisture for Gaussian surfaces, whereas exponential surfaces do not show the same behavior.

Backscatter averaging shows least errors in nearly all cases for the lowest surface correlation lengths considered ($kl = 2.4$) for both surface correlation types; $\Delta\sigma_0 < 0.6$ dB in the case of heterogeneous moisture, and $\Delta\sigma_0 < 3$ dB in the case of heterogeneous roughness. For medium and long correlation lengths ($kl \geq 4.8$), it is seen that for high-contrast pixels, the average values are always lower than the “true” backscattering coefficients. This implies that if the averaging assumption is used for soil moisture inversion, the value of soil moisture will always be underestimated, the quantification of which is a suitable subject for future study.

V. CONCLUSION

We find that the applicability of the backscatter averaging assumption for bare surfaces depends critically on the heterogeneous contrast, the type of heterogeneity, the surface correlation type, and the correlation length in ways that have been thus far described.

In a field work campaign that investigated the use of L-band SAR data for estimating soil moisture and roughness parameters [12], measurements of a number of different surfaces were made to quantify the surface statistics. The autocorrelation function can be generalized to the form $\rho_n(x/l) = \exp(-|x/l|^n)$, where n is an experimentally determined parameter that gives exponential and Gaussian surfaces for $n = 1$ and 2, respectively. The study found that 76% of the surfaces could be described by $1 \leq n \leq 1.4$, i.e., closer to exponential surfaces, whereas the remaining fraction, corresponding to $1.5 \leq n \leq 2$, were closer to Gaussian surfaces.

As our results show, depending on the type of heterogeneity and contrast, the averaging assumption can break down for one or both correlation types with increasing correlation lengths. The breakdown is more severe for Gaussian correlated surfaces,

which, while being in the minority, still constitute a significant fraction of surfaces.

To our knowledge, this is the first systematic theoretical study that examines the validity of the backscatter averaging assumption. Based on our findings, we recommend that measurement of surface correlation type and length be made an integral part of remote-sensing fieldwork campaigns. Scalar averaging of backscatter is a widespread practice in remote sensing, and in the absence of information regarding correlation type or length, there can be little theoretical basis for claiming accuracy to the act of averaging.

Our study highlights conditions under which this averaging is accurate and when it will fail. In the cases that it does fail, it would be more appropriate to obtain an average soil moisture value for a pixel by averaging inverted soil moisture values of constitutive pixels, rather than taking the average of backscattering coefficients and inverting this value to get an average soil moisture values. Future work will investigate disaggregation of coarse-scale pixels to allow soil moisture radar retrievals at fine-scale resolution, which can then be aggregated to determine coarse-scale soil moisture.

REFERENCES

- [1] E. Chapin, A. Chau, J. Chen, B. Heavey, S. Hensley, Y. Lou, R. Machuzak, and M. Moghaddam, “AirMOSS: An Airborne P-band SAR to measure root-zone soil moisture,” in *Proc. IEEE RADAR Conf.*, 2012, pp. 0693–0698.
- [2] D. Entekhabi, E. Njoku, P. O’Neill, K. Kellogg, W. Crow, W. Edelstein, J. Entin, S. Goodman, T. Jackson, J. Johnson, J. Kimball, J. Piepmeier, R. Koster, N. Martin, K. McDonald, M. Moghaddam, S. Moran, R. Reichle, J. Shi, M. Spencer, S. Thurman, L. Tsang, and J. Van Zyl, “The soil moisture active passive (SMAP) mission,” *Proc. IEEE*, vol. 98, no. 5, pp. 704–716, May 2010.
- [3] M. Burgin and M. Moghaddam, “Investigating spatial aggregation techniques using a heterogeneous radar landscape simulator for reducing uncertainties of soil moisture retrieval from SMAP,” in *Proc. IEEE IGARSS*, 2011, pp. 265–268.
- [4] S. Huang, L. Tsang, E. G. Njoku, and K. S. Chan, “Backscattering coefficients, coherent reflectivities, and emissivities of randomly rough soil surfaces at L-band for SMAP applications based on numerical solutions of Maxwell equations in three-dimensional simulations,” *IEEE Trans. Geosci. Remote Sens.*, vol. 48, no. 6, pp. 2557–2568, Jun. 2010.
- [5] U. K. Khankhoje, J. J. van Zyl, and T. A. Cwik, “Computation of radar scattering from heterogeneous rough soil using the finite-element method,” *IEEE Trans. Geosci. Remote Sens.*, vol. 51, no. 6, pp. 3461–3469, Jun. 2013.
- [6] D. Riley, J.-M. Jin, Z. Lou, and L. Petersson, “Total-and scattered-field decomposition technique for the finite-element time-domain method,” *IEEE Trans. Antennas Propag.*, vol. 54, no. 1, pp. 35–41, Jan. 2006.
- [7] A. F. Oskooi, L. Zhang, Y. Avniel, and S. G. Johnson, “The failure of perfectly matched layers, and towards their redemption by adiabatic absorbers,” *Opt. Exp.*, vol. 16, no. 15, pp. 11 376–11 392, Jul. 2008.
- [8] U. K. Khankhoje and T. A. Cwik, “A mesh reconfiguration scheme for speeding up Monte Carlo simulations of electromagnetic scattering by random rough surfaces,” *Comput. Phys. Commun.*, vol. 185, no. 2, pp. 445–447, Feb. 2014.
- [9] N. Peplinski, F. Ulaby, and M. Dobson, “Dielectric properties of soils in the 0.3–1.3-GHz range,” *IEEE Trans. Geosci. Remote Sens.*, vol. 33, no. 3, pp. 803–807, May 1995.
- [10] S. O. Rice, “Reflection of electromagnetic waves from slightly rough surfaces,” *Commun. Pure Appl. Math.*, vol. 4, no. 2/3, pp. 351–378, Aug. 1951.
- [11] F. T. Ulaby, R. K. Moore, and A. K. Fung, *Microwave Remote Sensing: Active and Passive—Volume 2*. Reading, MA, USA: Addison-Wesley, 1982.
- [12] J. Shi, J. Wang, A. Hsu, P. O’Neill, and E. T. Engman, “Estimation of bare surface soil moisture and surface roughness parameter using L-band SAR image data,” *IEEE Trans. Geosci. Remote Sens.*, vol. 35, no. 5, pp. 1254–1266, Sep. 1997.